A&A 477, 139–145 (2008)
DOI: 10.1051/0004-6361:20078392

Astronomy & Astrophysics

Candidate Milky Way satellites in the Galactic halo

C. Liu[1,2], J. Hu[1], H. Newberg[3], and Y. Zhao[1]

[1] National Astronomical Observatories, Chinese Academy of Sciences, Beijing 100012, PR China
e-mail: chaoliu@lamost.org
[2] Graduate University of Chinese Academy of Sciences, Beijing 100049, PR China
[3] Department of Physics, Applied Physics, and Astronomy, Rensselaer Polytechnic Institute, Troy, NY 12180, USA

Received 1 August 2007 / Accepted 28 September 2007

ABSTRACT

Aims. Sloan Digital Sky Survey (SDSS) DR5 photometric data with $120° < \alpha < 270°$, $25° < \delta < 70°$ were searched for new Milky Way companions or substructures in the Galactic halo.
Methods. Five candidates are identified as overdense faint stellar sources that have color-magnitude diagrams similar to those of known globular clusters, or dwarf spheroidal galaxies. The distance to each candidate is estimated by fitting suitable stellar isochrones to the color-magnitude diagrams. Geometric properties and absolute magnitudes are roughly measured and used to determine whether the candidates are likely dwarf spheroidal galaxies, stellar clusters, or tidal debris.
Results. SDSSJ1000+5730 and SDSSJ1329+2841 are probably faint dwarf galaxy candidates while SDSSJ0814+5105, SDSSJ0821+5608, and SDSSJ1058+2843 are very likely extremely faint globular clusters.
Conclusions. Follow-up study is needed to confirm these candidates.

Key words. Galaxy: structure – Galaxy: halo – galaxies: dwarf – Local Group

1. Introduction

The discovery of tidal streams in the Milky Way from the accretion of smaller galaxies supports hierarchical merging cosmogonies (Lynden-Bell & Lynden-Bell 1995). The large-scale tidal arms of the Sagittarius dwarf spheroidal galaxy accretion event were the first to be discovered (Yanny et al. 2003; Majewski et al. 2003; Rocha-Pinto et al. 2004), and more tidal streams continued to be detected in Sloan Digital Sky Survey (SDSS; York et al. 2000) data. The remarkably strong tidal tails of Palomar 5 were discovered by Odenkirchen et al. (2001), Rockosi et al. (2002), and Grillmair & Dionatos (2006a). Another tidal stream was connected with NGC 5466 (Belokurov et al. 2006a; Grillmair & Johnson 2006). Belokurov et al. (2006b) revealed the so-called *Field of Streams*, which shows not only Sagittarius arms but also the Virgo overdensity (Jurić et al. 2005), Monoceros Ring (Newberg et al. 2002), Orphan stream (Belokurov et al. 2006b; Grillmair 2006a), and a 60°-long stream between Ursa Major and Sextans (Grillmair & Dionatos 2006b). The fact that tidal streams are often associated with globular clusters or dwarf spheroidal galaxies implies that it is possible to search for tidal streams by identifying new faint satellite dwarf galaxies, globular clusters, or tidal debris and to ascertain their connections.

New satellite companions of the Milky Way have been discovered in recent years. About 150 globular clusters (Harris 1996) and 9 widely-accepted dwarf spheroidal galaxies (dSph) (Belokurov et al. 2007) were known before the SDSS. Since 2005, tremendous progress has been made using SDSS data; at least nine new companions were discovered within two years. Seven of them are dSph satellites: Ursa Major I (Willman et al. 2005a), Canes Venatici I (Zucker et al. 2006a), Boötes (Belokurov et al. 2006c), Ursa Major II (Zucker et al. 2006b; Grillmair 2006a), Coma Berenics, Canes Venatici II, Hercules, and Leo IV (Belokurov et al. 2007). Two of them are probably globular clusters: Willman 1 (Willman et al. 2005b) and Segue 1 (Belokurov et al. 2007).

It is impossible to see these objects in SDSS images since they are resolved into field stars. They were discovered by detecting local stellar overdensities in SDSS stellar databases (Belokurov et al. 2007) by adding constraints on magnitude and color index. Overdensity study is a quick data-mining method for finding previously unknown satellite galaxies or globular clusters. We use a method similar to that of Belokurov et al. (2006c), but utilize different parameters to scan an area of the sky bounded by $120° < \alpha < 270°$, $25° < \delta < 70°$, and to observe five interesting overdensities with color–magnitude diagrams similar to a globular cluster or a dSph. They can be candidate globular clusters, dSphs, or tidal debris.

The organization of this paper is as follows. Section 2 describes our methods of searching for candidates and measuring their properties. Data reduction processes, including the method for identifying candidates, are discussed in Sect. 2.1. A template-matching algorithm for estimating the distance to each overdensity is described in Sect. 2.2. A rough measurement of geometric properties and radial profiles are addressed in Sect. 2.3. In Sect. 3 we discuss the nature of each overdensity and a short conclusion is included in the last session.

2. Discovery

SDSS DR5 provides photometric data in u, g, r, i, and z passbands (Fukugita et al. 1996) and covers 8000 square degrees of sky (Adelman-McCarthy et al. 2007). We have selected only the objects with stellar profiles from SDSS databases. SDSS recognizes all point sources as stars, including quasars and faint galaxies. Thus, galaxy clusters and arms and halos of bright galaxies contaminate our sample of overdensities. In order to decrease the frequency of these contaminants, we used only sources with

magnitude $19 < i < 22$ and color $0 < g - i < 1$. We limited the area of sky searched to avoid the Sagittarius dwarf spheroidal galaxy's tidal arms. Approximately 3.6×10^7 point sources were obtained in the region $120° < \alpha < 270°$, $25° < \delta < 70°$ from SDSS Casjobs[1]. The magnitudes in each band were corrected for extinction using values provided by the SDSS database, which are computed following Schlegel et al. (1998).

2.1. Data reduction

Data analysis procedures were based on the China Virtual Observatory's experimental data access service (VO-DAS). We computed the star counts for this data in bins of size $0.2° \times 0.2°$; hence, 750×225 bins were generated. Field mean density and standard deviation for each bin were defined by the star counts in the surrounding bins, within a 11×11 window. The standard deviation was derived from all bins in the box except the center bin. The strength of the peak in the center bin was estimated from

$$\tilde{n}_{\rm center} = (n_{\rm center} - \mu)/\sigma, \quad (1)$$

where $n_{\rm center}$ is the number of stars in the center bin, μ the average number of stars per bin in the surrounding bins, and σ the standard deviation. For most objects, the bin size is large enough to contain an entire star cluster, and the surrounding bins contain many Galactic stars. For our sample, $\tilde{n}_{\rm center}$ is normally distributed with $\tilde{\mu} = 0.33$ and $\tilde{\sigma} = 0.56$. We selected all peaks with $\tilde{n}_{\rm center} > \tilde{\mu} + \mathbf{3}\tilde{\sigma} \sim \mathbf{2}$. From these statistics, we expect that about 0.27% of the bins we search will contain statistical fluctuations high enough to be detected as a peak. We searched 168 750 bins, of which we excluded 18 627 zero bins (sky areas which are not covered by SDSS). Therefore, we expect about 405 overdensities to be caused by field-star density fluctuation.

We actually identified 524 overdensity bins, which is 119 more than would be expected from statistics. The 524 overdensities include statistical fluctuations, previously identified Milky Way satellites, bright galaxies, bright stars, and galaxy clusters, in addition to the new Milky Way satellites we would like to find. We used additional information from the color-magnitude distribution of stars in the overdensities to cull out the statistical fluctuations, as described below. Known objects including bright galaxies, galaxy clusters, and bright stars are manually identified and eliminated. The known Milky Way satellites that were re-discovered by this technique include: UMa II, UMa I, Willman 1, Pal4, CVn II, CVn I, NGC 5272, NGC 5466, NGC 6205, NGC 6341, Draco, and Leo III, some of which cover more than 2 bins due to their large angular sizes. Overdensity bins that are close to the survey boundaries (within 0.5°) are also ignored.

Density contour diagrams and CMDs were generated within a $1° \times 1°$ area centered at the remaining overdensity bins. Candidates were manually identified by comparing the density contour diagram and CMD of each overdensities with those of 9 known objects: Pal 4, UMa I, UMa II, CVn I, Draco, NGC 6341, NGC 5466, Willman 1, and NGC 6205. The distance modulus (DM) of these templates ranges from 14.2 mag to 21.7 mag. This ensures that the templates cover all possible morphological features for a CMD, since the stellar populations that are probed within our magnitude limits depend on the distance modulus.

Five overdensities are finally chosen from over 500 initial candidates. Figure 1 displays density contours, core (circle with $r = 0.1°$ or $r = 0.15°$) CMDs, field (annuli area between $r = 0.5°$ and $r = 0.6°$) CMDs, and Hess diagrams (subtraction between corresponding center area CMDs and field CMDs with normalized star counts) for these five candidate Milky Way satellites.

[1] http://casjobs.sdss.org/dr5/en/

2.2. Distances to the overdensities

Distances to the five candidates were estimated by fitting isochrone lines to the CMD of each overdensity. An automatic template-matching algorithm was developed to discover the best-fit Padova isochrone lines (Giradi et al. 2004) for each candidate. Stellar evolution isochrone lines were converted to masks where the color index $g-i$ changed from -1 to 2 with step of 0.03 and the magnitude i changed from -10 to 10 with step of 0.1. Thus a binary 100×200 image mask for each isochrone line was formed. The value of each pixel in the image is either 1 (in the neighborhood of an isochrone line) or 0 (everywhere else). A series of mask templates were created for a range of metallicity, age, and distance moduli. For each candidate, the template that minimizes R, as defined by the following formula, was selected as the best match.

$$R = \frac{\sum\limits_{g-i,i} (C(g-i,i)(1 - T(g-i,i,Z,A,DM)))}{\sum\limits_{g-i,i} C(g-i,i)} \quad (2)$$

where $C(g-i,i)$ is the candidate's Hess diagram ($i = 13{-}22$ mag), $T(g{-}i,i,Z,A,DM)$ is a template mask with specific metallicity Z, age A, and distance modulus DM. The value of Z is 0.0001, 0.0004, 0.001, or 0.004. The value of A, in $\log_{10}$(yr), ranges from 9.5 to 10.25 with a step of 0.05. And the value of DM ranges from 13 mag to 21.9 mag with a step of 0.1 mag. In total, 5760 templates were evaluated for each overdensity. The value of R also measures the goodness of the fit. The smaller R, the better the fit.

The minimum value of R, $R_{\rm min}$, measures how many stars, in percent, are unrelated to the best fit isochrone line in the Hess diagrams. In the extreme case where stars are uniformly distributed in the color–magnitude plane, considering that the isochrone line is only a thin line and cannot cover many stars in the plane, $R_{\rm min} \sim 1$ is derived. In the opposite extreme case where the candidate contains no background stars so that its features are completely described by a template, $R_{\rm min} \sim 0$ is reasonable. The $R_{\rm min}$ distributions for all known objects, candidates satellites, and other overdensities are shown in Fig. 2. The population of known objects and candidates addresses significantly lower $R_{\rm min}$ values than that of non-candidates overdensities.

Specifically, we used 9 known globular clusters and dwarf spheroidal galaxies – UMa I & II, CVn I & II, Pal4, NGC 6205, NGC 5466, NGC 5272, and NGC 6341 – to test the effectiveness of the algorithm. They are all located in the detected area and were all detected by our selection process. Their distance moduli range from 14 to 22, as measured by previous authors (listed in Table 1). The standard deviation in the accuracy of the DM is $\sigma = 0.23$ mag.

Best-fit isochrone lines are shown together with Hess diagrams of our candidate Milky Way satellites in Fig. 3. The distance modulus of the best-fit template is an estimate of the distance to each overdensity. Table 2 displays the parameters of the matching templates for each candidates although we do not expect that this method of isochrone fitting will produce accurate measurements of the ages and metallicities of each candidate. We list our best-fit metallicity and age parameters simply

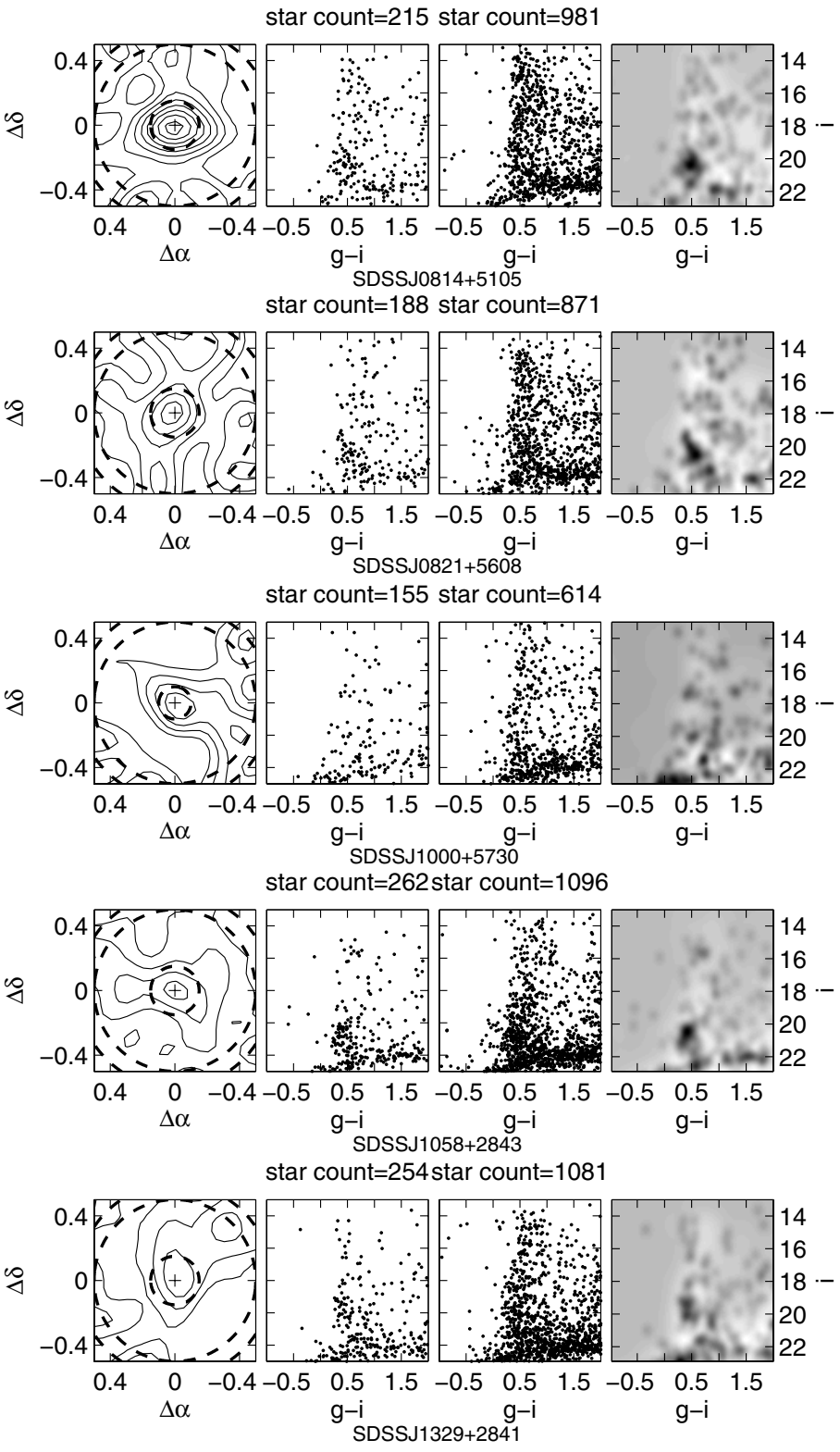

Fig. 1. Overdensity detections. The first column of diagrams are density contours. Each density contour is constructed by a nonparametric distribution density estimation with a Gaussian kernel and a window width of 0.1°, using stars with $19 < i < 22$ mag located in the $1° \times 1°$ area around the candidate. The second column of diagrams displays the core CMDs of overdensities. Points in this column are samples from the smallest circle ($r = 0.1°$ or $0.15°$) overlaid on density contours. The third column of diagrams displays field CMDs of the overdensities. Points in this column are samples from the annuli between the intermediate circle ($r = 0.5°$) and the biggest circle ($r = 0.6°$). The most right column of diagrams shows Hess diagrams that are the result of subtraction between the core CMDs and corresponding field CMDs with normalization on total star counts. The size of each bin in the Hess diagrams is 0.03 mag × 0.1 mag.

to show that they are not unreasonable for star clusters or dwarf galaxies in the Galactic halo.

The $R_{\rm min}$ values in Table 1 again show the same trend with Fig. 2 that globular clusters have lower $R_{\rm min}$ values, while low surface-brightness dSphs (for example UMa II) have higher $R_{\rm min}$ values. The fact that an acceptable DM is derived for UMa II, although it has a higher $R_{\rm min}$ that reaches the non-candidate range(see Fig. 2), gives us confidence that our technique for finding distances is valid even for these low surface-brightness candidates.

2.3. Properties of candidates

Center positions, geometric properties, and absolute magnitudes were estimated for each candidate and listed in Table 2.

Table 1. Comparison of distances from template matching method with previous studies.

Name	Z from template	Age from template ($\log_{10}$(yr))	DM from template (mag)	DM from references (mag)	$R_{\rm min}$	References
UMa II	0.0004	10.1	17.9	17.5	0.50	Zucker et al. (2006b)
UMa I	0.0001	10	19.9	20	0.41	Willman et al. (2005a)
Pal4	0.001	10.2	20.2	20.02	0.37	Harris (1996)
CVn II	0.0004	10.2	20.9	20.9	0.25	Belokurov et al. (2007)
CVn I	0.0004	10.15	21.7	21.75	0.28	Zucker et al. (2006a)
NGC 5272	0.001	10.1	15	15.04	0.21	Harris (1996)
NGC 5466	0.001	10.05	16.1	16.1	0.34	Harris (1996)
NGC 6205	0.004	9.95	14.7	14.28	0.21	Harris (1996)
NGC 6341	0.001	10	14.9	14.59	0.28	Harris (1996)

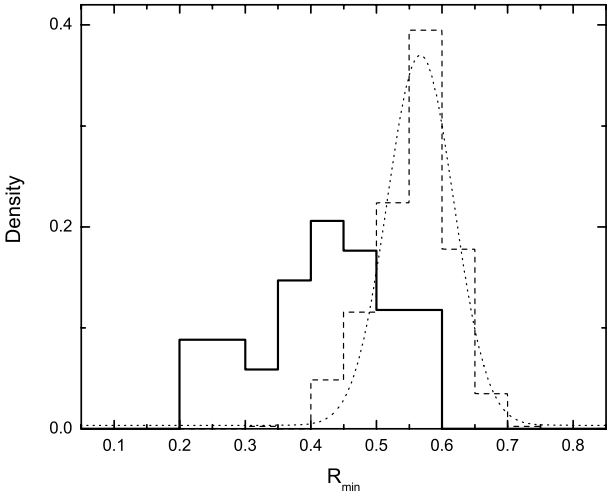

Fig. 2. Comparison of $R_{\rm min}$ for real objects compared with all original two sigma detections. Two populations of $R_{\rm min}$ values distribution are displayed. The solid stair line shows all known objects, including globular clusters, dwarf galaxies, bright galaxies, and galaxy clusters, and our five candidates. The distribution shows two peaks. The peak between 0.2 and 0.3 is due to 5 known globular clusters. The peak at 0.4 is associated with dwarf galaxies and normal galaxies. As comparison, the dashed stair line shows the distribution of all other overdensities with a Gaussian fitting curve (dot line), where the average value is $R_{\rm min} = 0.57$ and $\sigma = 0.1$. This figure shows that the globular clusters have the smallest $R_{\rm min}$, the dwarf galaxies reach a larger radius, and both objects have a significantly smaller $R_{\rm min}$ than non-candidates.

To measure position and geometric properties for each candidate Milky Way satellite, stars associated with candidates were selected. We selected stars that are located within the $1^\circ \times 1^\circ$ around the center position of candidates and also within bins in the Hess diagram (right panel in Fig. 1) that have more than 0.05 stars per bin. Density contour diagrams of the five candidates were derived by counting selected stars and are displayed in Fig. 4.

Because there are relatively few stars in our samples, we did not fit for the ellipticity of the candidates. We fit only circularly symmetric profiles. The background level was estimated by averaging star density of an annulus area around each candidate with a radius from 30 arcmin to 60 arcmin. It is then subtracted from radial profile before fitting.

To check our methods, we compared the half-light radius of Pal5 and Boo using our method and compared the results with previous measurements in the literature. For Pal5, we derived $r_{\rm h} = 2.64' \pm 0.07$ for the exponential model and $r_{\rm h} = 2.91' \pm 0.07$ for the Plummer model. These values are similar to the previously measured value of $r_{\rm h} = 2.96'$ in Harris (1996). For Boo, we found $r_{\rm h} = 14.4' \pm 1.8$ for the exponential model and $r_{\rm h} = 14.6' \pm 1.5$ for the Plummer model, while corresponding values are $r_{\rm h} = 13.0' \pm 0.7$ and $r_{\rm h} = 12.6' \pm 0.7$ in Belokurov et al. (2006c). The results support our methods for estimating globular cluster and dwarf galaxy parameters, though there may be larger errors for lower luminosity objects. All candidates are fitted by exponential and Plummer models (McConnachie & Irwin 2006). Radial profiles and fitting curves are displayed in Fig. 5. Half-light radii derived by integrating exponential and Plummer profiles are tabulated in Table 2. Geometrical sizes of these candidates were computed from the estimated distances and the angular sizes from each model profile, and are shown in Table 2.

To estimate absolute magnitude of candidates we used Hess diagrams derived by subtracting field Hess diagrams from those generated by stars inside $r_{\rm h}$, normalized by area. By overlapping corresponding best-matched isochrone masks on these Hess diagrams, only star counts located at neighbors of isochrone lines are kept. Then, g-band and r-band magnitudes are computed by integrating all positive flux values in these masked Hess diagrams. Total color index $(B-V)_{\rm tot}$ and Total apparent magnitude $V_{\rm tot}$ were conducted from Eqs. (3) and (4) (Fukugita et al. 1996):

$$(B-V)_{\rm tot} = (g_{\rm tot} - r_{\rm tot} + 0.23)/1.05 \quad (3)$$

$$V_{\rm tot} = r_{\rm tot} + 0.49(B-V)_{\rm tot} - 0.11 \quad (4)$$

$$M_{V,\rm tot} = V_{\rm tot} + 5 - 5\log(d). \quad (5)$$

Consequently, absolute magnitudes are computed via Eq. (5). Absolute magnitudes estimated with different radial profile models are tabulated in Table 2. As a test, we estimated the absolute magnitudes of Com, CVn II, Her, and Leo IV, which are low luminosity dwarf galaxies discovered in SDSS data (Belokurov et al. 2007), using this method. The maximum bias of all four objects between our results and the literature's is $|\Delta M_{V,\rm tot}| = 0.55$ mag, which is smaller than the standard error (0.6 mag) mentioned in the literature. ANOVA analysis also shows that the estimation of our method is not significantly different from those from Belokurov et al. (2007).

3. Discussion

It is difficult to identify all 5 candidates reliably using only SDSS data; accurate follow up observations using a large telescope are required to determine the types, which could be star clusters, dwarf spheroidal galaxies, tidal debris, or the chance superposition of field stars. We expect that these candidates are not merely field stars.

Table 2. Parameters of each overdensity.

Parameter	SDSSJ0814+5105	SDSSJ0821+5608	SDSSJ1000+5730	SDSSJ1058+2843	SDSSJ1329+2841
RA (J2000)	$08^h13^m42^s$	$08^h21^m15^s$	$10^h00^m28^s$	$10^h58^m04^s$	$13^h29^m13^s$
Dec (J2000)	$+51°05'27''$	$+56°08'16''$	$+57°30'10''$	$+28°42'39''$	$+28°41'27''$
l (deg)	167.743	161.665	155.506	202.649	45.716
b (deg)	33.449	34.615	47.372	64.966	81.513
Z	0.004	0.004	0.001	0.004	0.0004
Age ($\log_{10}$(yr))	10.05	10	10.15	9.95	10.1
$(m-M)_0$ (mag)	15.7	15.7	19.6	16.9	19.4
$R_{\min}$	0.5	0.45	0.47	0.36	0.58
Distance (kpc)	$13.8^{+1.5}_{-1.4}$	$13.8^{+1.5}_{-1.4}$	$83.2^{+9.3}_{-8.4}$	$24^{+2.7}_{-2.4}$	$75.9^{+8.5}_{-7.6}$
r_h (exponential) (arcmin)	6.2 ± 1.0	4.7 ± 1.0	8.1 ± 2.7	4.7 ± 0.7	8.6 ± 2.5
r_h (Plummer) (arcmin)	5.4 ± 0.8	4.3 ± 0.8	8.3 ± 2.2	4.8 ± 0.5	8.8 ± 1.9
$r_{h,g}$ (exponential) (pc)	24.9 ± 4.0	18.9 ± 4.0	196.0 ± 63	32.8 ± 4.9	189.8 ± 55
$r_{h,g}$ (Plummer) (pc)	21.7 ± 3.2	17.3 ± 3.2	200.8 ± 53	33.5 ± 3.5	194.2 ± 42
Background level (arcmin^{-2})	0.11	0.1	0.02	0.12	0.12
M_V (exponential) (mag)	–0.77	–1.63	–4.15	–2.99	–3.91
M_V (Plummer) (mag)	–0.81	–1.42	–4.16	–2.98	–3.92

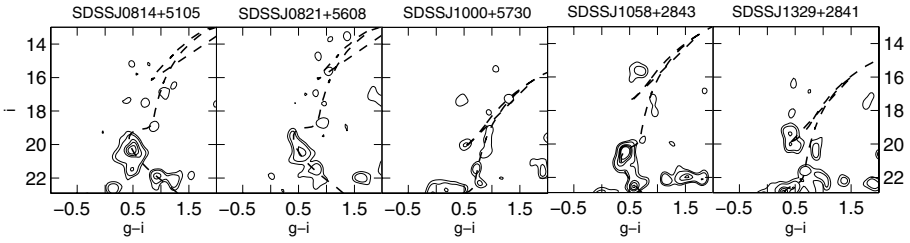

Fig. 3. The Hess contours of candidates with the best-fitting isochrone lines overlaid on them. Contours are positive densities (0.05, 0.1, 0.15, 0.2, 0.25, 0.3 stars per bin). The size of each bin is 0.03 mag × 0.1 mag. Best-fitting stellar evolution isochrone lines are overlaid with dashed lines.

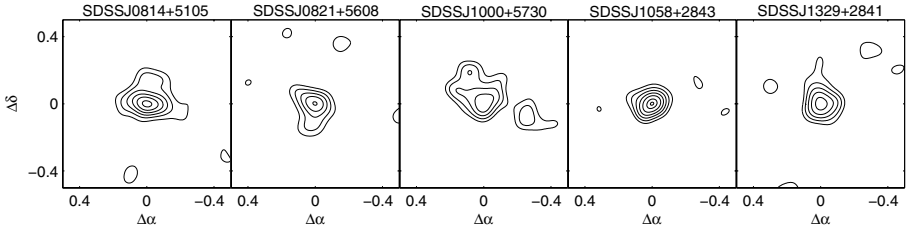

Fig. 4. Isodensity contours of five candidates. The contour levels are 2, 3, 4, 5, 6, 7, and 7.5σ above the background. The samples that generate the contours are selected from the corresponding Hess diagram.

Belokurov et al. (2007) uses the R_h vs. M_V plane to identify Her, Leo IV, CVn II, Com as dSphs, while Seg I is an unusual, low- luminosity globular cluster. We adopt the same method, and plot our candidates with known Milky Way satellites in Fig. 6. The half-light radii of 5 candidates were derived by integrating exponential profiles and Plummer profiles. The absolute magnitudes were derived by adding all possible member stars flux that are located in a half-light radius and time 2. We plot the 5 candidates in the R_h vs. M_V plane with the mean values derived by exponential and the Plummer model. Both R_h and M_V of known globular clusters come from Harris (1996), and those of SDSS-discovered Milky Way dwarf spheroidal galaxies come from Belokurov et al. (2006c), Belokurov et al. (2007), Zucker et al. (2006b), Willman et al. (2005a), and Willman et al. (2005b). Those dwarf galaxies in the local group come from Irwan & Hatzidimitriou (1995) and Mateo (1998), and those Andromeda dwarf galaxies come from McConnachie & Irwan (2006) and Martin et al. (2006).

SDSSJ0814+5105, SDSSJ0821+5608, and SDSSJ1058+2843 have surface brightness similar to other known satellites discovered from the SDSS with extremely faint absolute magnitudes, even fainter than AM4, the faintest one in Harris 1996). Their location in Fig. 6 suggests that these stellar systems are more like globular clusters than dwarf galaxies. Tidal radii of SDSSJ0814+5105, SDSSJ0821+5608, and SDSSJ1058+2843 in Fig. 6 are computed using the equation

$$r_{\rm tidal} \sim R\left(\frac{M_{\rm cand}}{3M_{\rm MW}}\right)^{1/3} \quad (6)$$

from Binny & Tremaine (1987), where R is the candidate's galactocentric distance, $M_{\rm cand}$ is its total mass, and $M_{\rm MW}$ is the total mass of the Milky Way within R. We assume that the distance from the Sun to the center of the Milky Way is 8 kpc and $v_c = 220$ km s^{-1} at distance R. The value of $M_{\rm cand}$ was estimated by comparing star counts of F and G stars located in main sequences of the three candidates and Pal 5 (Fig. 7). Since the formula for the tidal radius does not include dark matter, the actual tidal radius is larger than estimated if the candidates are dwarf galaxies with substantial dark matter content.

Notice that SDSSJ0814+5105 and SDSSJ0821+5608 overlap the anticenter stream (Grillmair 2006b), which may be related to Monoceros Ring displayed in Fig. 8. According to Newberg et al. (2002) the turnoff magnitude of Monoceros Ring is at $g = 19.4$. In Fig. 1 we estimate the SDSSJ0814+5105 and SDSSJ0821+5608 have a magnitude of the turnoff as $g = 19.5$. They are almost at the same distance. However, according to Grillmair (2006b), the anticenter stream has a turnoff magnitude as $g = 18.7$, quite different from the results of

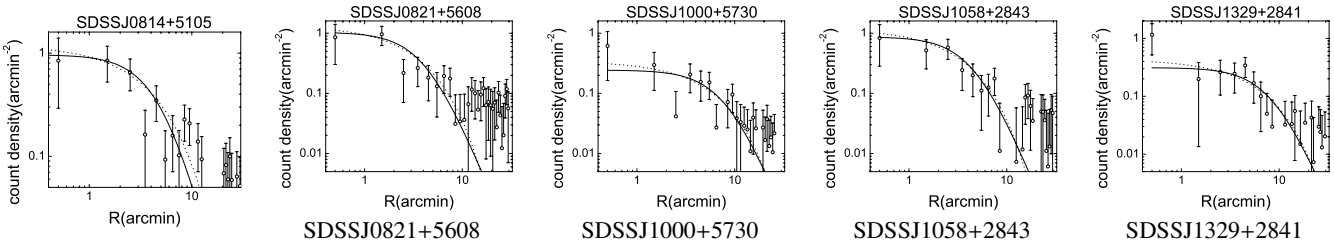

Fig. 5. Density radial profiles for candidates. Background levels are subtracted before fitting models. The solid lines are Plummer model fit curves. The dashed lines are exponential model fit curves.

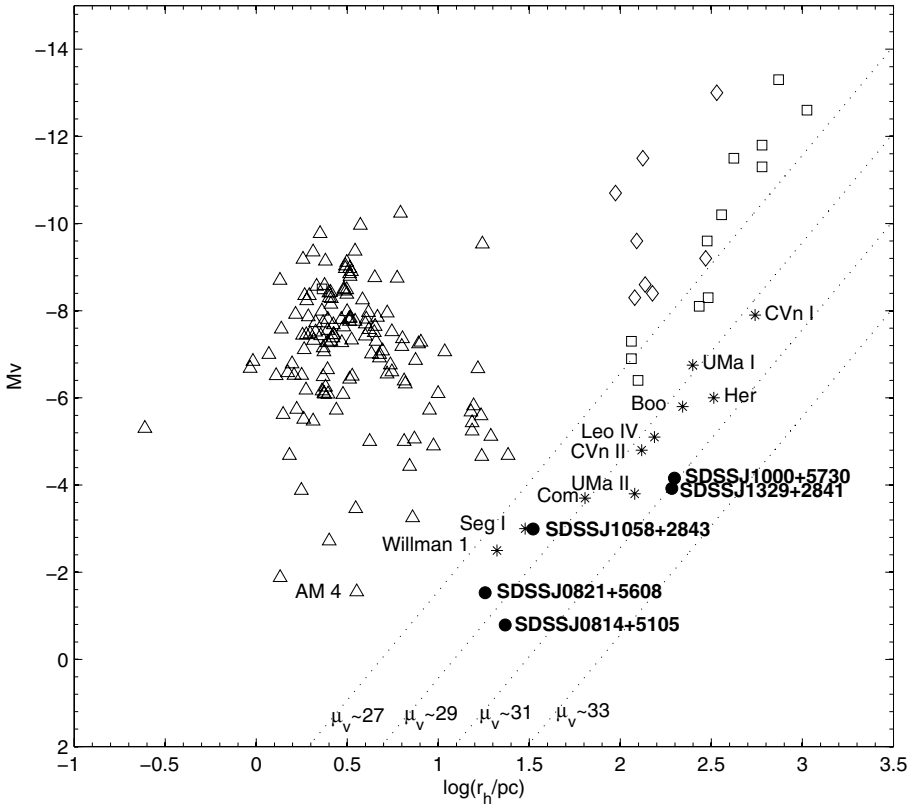

Fig. 6. Location of different classes of objects in the plane of half light radius vs. absolute magnitude. Lines of constant surface brightness are marked. Filled circles with bold labels are the 5 candidates revealed in this paper. Triangles are known globular clusters (Harris 1996). Stars with labels are Milky Way satellites discovered from SDSS (Belokurov et al. 2006c, 2007; Zucker et al. 2006b; Willman et al. 2005a,b), Diamonds are dwarf galaxies in the local group (Irwan & Hatzidimitriou 1995; and Mateo 1998). Rectangles are Andromeda dwarf galaxies (McConnachie & Irwan 2006; Martin et al. 2006).

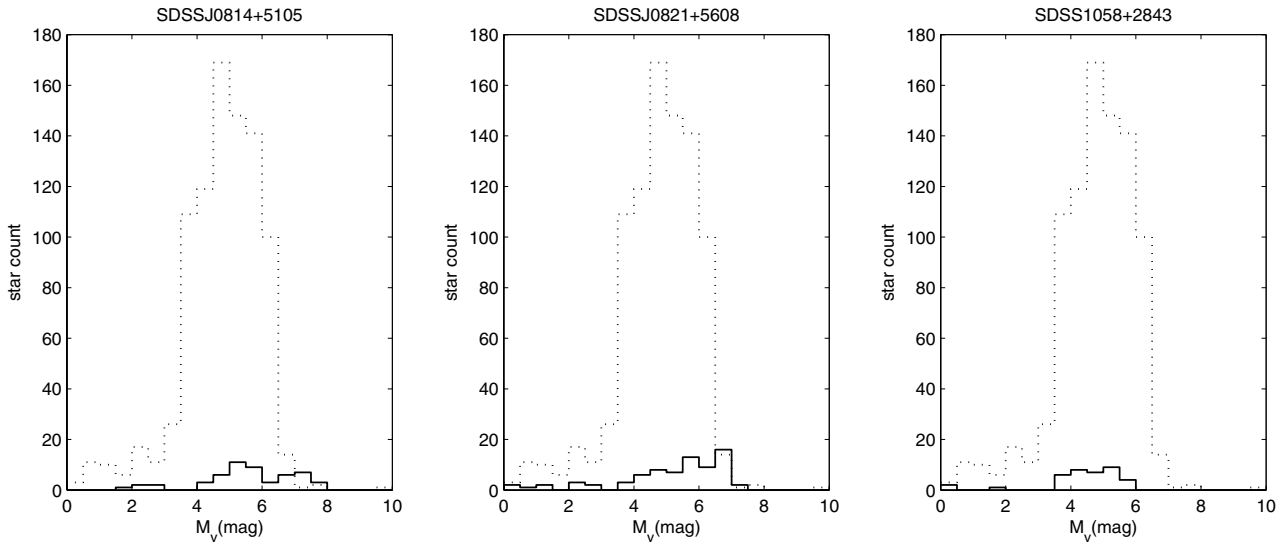

Fig. 7. Luminosity function comparison between SDSSJ0814+5105, SDSSJ0821+5608, and SDSSJ1058+2843, marked as solid line, and Pal 5, marked as a doted line, within half-light radii. Stars between 4 and 6 mag correspond to spectral types from F to G in main sequence. Star counts of F and G stars are used to roughly estimate the total mass.

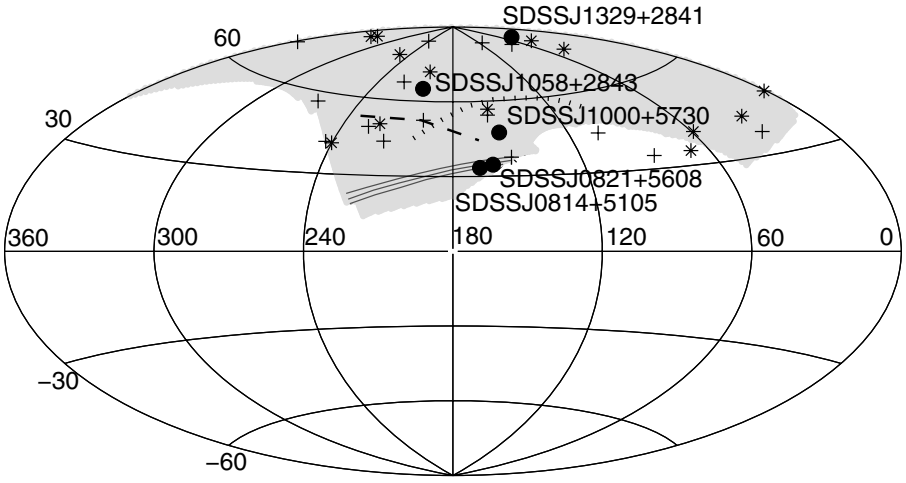

Fig. 8. Overdensities' positions in galactic coordinates in Aitoff projection. The gray area encloses the main area of the North Galactic Cap covered by the SDSS DR5 data. Filled circles are candidates in this paper. Plus symbols are UMa II, Willman 1, UMa I, CVn I, CVn II, Her, Leo IV, Com, and Seg 1. Star symbols are globular clusters in the SDSS DR5 area we detect. The triple thin solid lines are Anticenter Stream of Grillmair (2006b), which may be related to the Monoceros Ring. The thin dotted line is GD-1. The thin dashed line is Orphan stream.

Newberg et al. (2002) and substantially closer than the new candidates. The question is whether they are globular clusters in the Monoceros stream or just part of the debris but more compact than in other areas?

SDSSJ1000+5730 and SDSSJ1329+2841 are faint, extended objects with half-light radii similar to those of most of dSphs. They have a surface brightness near $\mu_V \sim 31$ mag/arcsec^2, which is lower than all known dSphs discovered from SDSS. Their type cannot be determined solely by the SDSS due to their faintness, but they look like dwarf galaxies.

4. Conclusions

In this paper we report five interesting overdensities detected in the SDSS database. They show features of globular clusters or dSphs in their CMDs. Mass estimation for SDSSJ0814+5105, SDSSJ0821+5608, and SDSSJ1058+2843 indicates that their tidal radii are bigger than their half-light radius, which implies that they are likely globular clusters with low surface brightness. The half-light radius and absolute magnitude of SDSSJ1329+2841 suggest a likely dSph. Although surface-magnitude measurements suggest that SDSSJ1000+5730 is fainter than all known dSphs, its Hess diagram implies that it is an interesting object that needs follow-up observations.

Acknowledgements. H.N. acknowledges funding from the National Science foundation (AST 07-33161). Funding for the SDSS and SDSS-II has been provided by the Alfred P. Sloan Foundation, the Participating Institutions, the National Science Foundation, the US Department of Energy, the National Aeronautics and Space Administration, the Japanese Monbukagakusho, the Max Planck Society, and the Higher Education Funding Council for England. The SDSS Web Site is `http://www.sdss.org/`.

The SDSS is managed by the Astrophysical Research Consortium for the Participating Institutions. The Participating Institutions are the American Museum of Natural History, Astrophysical Institute Potsdam, University of Basel, University of Cambridge, Case Western Reserve University, University of Chicago, Drexel University, Fermilab, the Institute for Advanced Study, the Japan Participation Group, Johns Hopkins University, the Joint Institute for Nuclear Astrophysics, the Kavli Institute for Particle Astrophysics and Cosmology, the Korean Scientist Group, the Chinese Academy of Sciences (LAMOST), Los Alamos National Laboratory, the Max-Planck-Institute for Astronomy (MPIA), the Max-Planck-Institute for Astrophysics (MPA), New Mexico State University, Ohio State University, University of Pittsburgh, University of Portsmouth, Princeton University, the United States Naval Observatory, and the University of Washington.

References

Adelman-McCarthy, J., et al. 2007, ApJS, in press
Binney, J., & Tremaine, S. 1987, Galactic Dynamics (Princeton: Princeton Univ. Press)
Belokurov, L., Evans, N. W., Irwin, M. J., Hewett, P. C., & Wilkinson, M. I. 2006a, ApJ, 637, L29
Belokurov, L., Zucker, D. B., Evans, N. W., et al. 2006b, ApJ, 642, L137
Belokurov, L., Zucker, D. B., Evans, N. W., et al. 2006c, ApJ, 647, L111
Belokurov, L., Zucker, D. B., Evans, N. W., et al. 2007, ApJ, 654, 897
Bergbusch, P. S., & VandenBerg, D. A. 1992, ApJS, 81, 163
Cox, A. N. 2000, Allen's Astrophysical Quantities, 4th edition (New York: Springer-Verlag Inc.), 400
Fukugita, M., Ichikawa, T., Gunn, J. E., et al. 1996, AJ, 111, 1748
Fellhauer, M., et al. 2006, MNRAS, submitted [arXiv:astro-ph/0611157]
Grillmair, C. J. 2006a, ApJ, 645, L37
Grillmair, C. J. 2006b, ApJ, 651, L29
Grillmair, C. J., & Smith, G. H. 2001, AJ, 122, 3231
Grillmair, C. J., & Dionatos, O. 2006a, ApJ, 641, L37
Grillmair, C. J., & Dionatos, O. 2006b, ApJ, 643, L17
Grillmair, C. J., & Johnson, R. 2006, ApJ, 639, L17
Girardi, L., Grebel, E. K., Odenkirchen, M., & Chiosi, C. 2004, A&A, 422, 205
Harris, W. E. 1996, AJ, 112, 1487
Irwin, M., & Hatzidimitriou, D. 1995, MNRAS, 277, 1354
Jurić, M., et al. 2005, ApJ, submitted [arXiv:astro-ph/0510520]
King, I. 1962, AJ, 67, 471
Lee, Y.-W., Demarque, P., & Zinn, R. 1990, ApJ, 350, 155
Lynden-Bell, D., & Lynden-Bell, R. M. 1995, MNRAS, 275, 429
Majewski, S. R., Skrutskie, M. F., Weinberg, M. D., & Ostheimer, J. C. 2003, ApJ, 599, 1082
Mandushev, G., Spassova, N., & Staneva, A. 1991, A&A, 252, 94
Martin, N., Ibata, R. A., Irwin, M. J., et al. 2006, MNRAS, 371, 1983
Mateo, M. L. 1998, ARA&A, 36, 435
McConnachie, A. W., & Irwin, M. J. 2006, MNRAS, 365, 1263
Newberg, H. J., Yanny, B., Rockosi, C., et al. 2002, ApJ, 569, 245
Odenkirchen, M., Grebel, E. K., Rockosi, C. M., et al. 2001, ApJ, 548, L165
Rocha-Pinto, Majewski, S. R., Skrutskie, M. F., Crane, J. D., & Patterson, R. J. 2004, ApJ, 615, 732
Rockosi, C. M., et al. 2002, AJ, 124, 349
Schlegel, D. J., Finkbeiner, D. P., & Davix, M. 1998, ApJ, 500, 525
Stetson, P. B., Bolte, M., Harris, W. E., et al. 1999, AJ, 117, 247
Willman, B., Dalcanton, J. J., Martinez-Delgado, D., et al. 2005a, ApJ, 626, L85
Willman, B., Blanton, M. R., West, A. A., et al. 2005b, AJ, 129, 2692
Yanny, B., Newberg, H. J., Grebel, E. K., et al. 2003, ApJ, 588, 824
York, D. G., Adelman, J., Anderson, J. E., Jr., et al. 2000, AJ, 120, 1579
Zucker, D. B., Kniazev, A. Y., Bell, E. F., et al. 2004, ApJ, 612, L121
Zucker, D. B., Belokurov, V., Evans, N. W., et al. 2006a, ApJ, 643, L103
Zucker, D. B., Belokurov, V., Evans, N. W., et al. 2006b, ApJ, 650, L41